

GATSBI: An Online GTSP-Based Algorithm for Targeted Surface Bridge Inspection

Kevin Yu

Harnaik Dhama

Kartik Madhira

Pratap Tokekar

Abstract—We study the problem of visually inspecting the surface of a bridge using an Unmanned Aerial Vehicle (UAV) for defects. We do not assume that the geometric model of the bridge is known. The UAV is equipped with a LiDAR and RGB sensor that is used to build a 3D semantic map of the environment. Our planner, termed *GATSBI*, plans in an online fashion a path that is targeted towards inspecting all points on the surface of the bridge. The input to *GATSBI* consists of a 3D occupancy grid map of the part of the environment seen by the UAV so far. We use semantic segmentation to segment the voxels into those that are part of the bridge and the surroundings. Inspecting a bridge voxel requires the UAV to take images from a desired viewing angle and distance. We then create a Generalized Traveling Salesperson Problem (GTSP) instance to cluster candidate viewpoints for inspecting the bridge voxels and use an off-the-shelf GTSP solver to find the optimal path for the given instance. As more parts of the environment are seen, we replan the path. We evaluate the performance of our algorithm through high-fidelity simulations conducted in Gazebo. We compare the performance of this algorithm with a frontier exploration algorithm. Our evaluation reveals that targeting the inspection to only the segmented bridge voxels and planning carefully using a GTSP solver leads to more efficient inspection than the baseline algorithms.

I. INTRODUCTION

Unmanned Aerial Vehicles (UAVs) are increasingly being used for visual coverage tasks such as environmental monitoring [1]–[3], surveillance [4], precision agriculture [5], [6], search and rescue [7], [8], and bridge inspection [9]–[16]. In this paper, we focus on the task of using UAVs for inspecting the surface of a bridge for defects such as corrosion, rust, fatigue, cracks, etc. that can be inspected visually, Figure 1. While UAVs are being used for bridge inspection, most operations are manual [17]. This requires skillful piloting in high wind conditions. Besides navigational challenges, visual inspection also requires careful planning of the viewpoints to obtain high-resolution images covering all points on the surface of the bridge. This is challenging to do manually for a large bridge where one may not always have visual-line-of-sight. To overcome these issues, our group has been developing solutions for assisting manual flights for targeted bridge inspection [18]. In this paper, we focus in particular on the issue of careful planning of inspection paths for the UAV to ensure high-resolution images for all points on the surface of the bridge.

Yu is with the Department of Electrical & Computer Engineering, Virginia Tech, U.S.A. Email: klyu@vt.edu Dhama, Madhira, and Tokekar are with the Department of Computer Science & Engineering, University of Maryland, U.S.A. {dhama, kmadhira, tokekar}@umd.edu

This work is supported by the National Science Foundation under grant number 1840044.

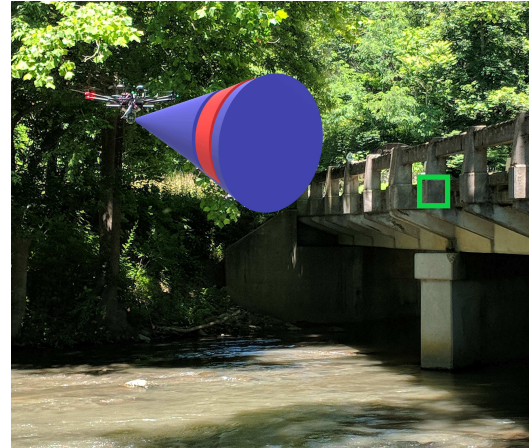


Fig. 1: An example of *viewP*. The green box represents the face of a bridge voxel, the blue cone represents the viewing cone, and the red band on the cone represents the viewing distance.

We say a point is inspected if at some point along the path of the UAV that point falls within the *viewing cone* and *viewing distance* of the camera attached to the UAV (defined in Section III). Our objective is to find a path of minimum length that guarantees inspection of all points on the surface of the bridge.

Inspection is closely related to coverage and exploration, problems that have been well-studied in the literature but, as we will show, are not necessarily the best approaches for inspection. If we are given a 3D model of the environment, (including the bridge), then we can find a coverage path that covers all points on the bridge using an offline planner [19]. In practice, we often do not have any prior model of the layout of the bridges. In many cases, even if a prior 3D model is available, it may not be accurate due to changes in the environment surrounding the bridge as well as structural changes that may have been made to the bridge. As a result, we focus on the more general problem of inspecting a bridge without any prior information about its geometry.

Frontier-based strategies [20] are typically used for exploring an initially unknown environment. A frontier is defined as the boundary between explored and unexplored regions. The strategies choose which amongst the set of frontiers to visit (and which path to follow to get to the chosen frontier) to help speed up exploration. The algorithm terminates when there are no more accessible unexplored regions. A bounding box can be placed around the bridge to restrict exploration

when operating in an open environment. Exploring the bridge does not necessarily mean that the UAV will get inspection quality images. Instead, an inspection planner that can take into account the viewing cone and distance constraints may be more efficient. We present such a planner, termed *GTSP-Based Algorithm for Targeted Surface Bridge Inspection (GATSBI)*, and show that it outperforms the frontier-based exploration strategies in terms of efficiently inspecting the bridge (Section V).

GATSBI consists of several modules: 3D occupancy grid mapping using LiDAR data, a semantic segmentation algorithm to find pixels that correspond to the surface of the bridge, a Generalized Traveling Salesperson Problem (GTSP) solver for finding inspection paths for the UAV, and a navigation algorithm for executing the planned path. We use off-the-shelf modules for occupancy grid mapping (Octomap [21]), solving GTSP (GLNS [22]), and point-to-point navigation (MoveIt [23]). Our key algorithmic contribution is to show *how* to reduce the inspection problem to a GTSP instance and the full pipeline that outperforms baseline strategies. Our technique takes into account overlapping viewpoints that can view the same parts of the bridge and simultaneously selects *where* to take images as well as *what order* to visit those locations. We also show when and how to replan as we obtain more information about the environment.

In summary, we make the following contributions:

- present an online algorithm, GATSBI, that plans paths to efficiently inspect bridges when no prior information about them is present;
- evaluate GATSBI (and the effects of various parameters within the algorithm) through numerous simulations in Gazebo using 3D models of bridges;
- compare GATSBI to a baseline frontier-based exploration algorithm using metrics that capture targeted inspection of bridges.

The rest of the paper is organized as follows. In Section II, we review previous work on inspection, coverage, and exploration. In Section III, we present the problem formulation and in Section IV, we describe our solution. In Section V, we present Gazebo simulation results. Finally, in Section VI we conclude with a discussion of future work.

II. RELATED WORK

As described earlier, frontier-based exploration is a widely-used method for 3D exploration of unknown environments [24]–[26]. Several variants of frontier exploration have been proposed, in particular, focusing on which amongst the frontiers to choose to visit next [27], [28]. Another popular approach is to model the exploration problem as that of information gathering and choosing a path (or a frontier) that maximizes the information gain [29], [30]. Additionally, there are Next-Best-View approaches [31] that, as the name suggests, plan the next-best location to take an image from in order to explore the environment. We refer the reader to a recent, comprehensive survey on multi-robot exploration by Quattrini-Li [32] that covers a variety of exploration strategies.

As we show in our simulations, generic exploration strategies are inefficient when performing targeted inspection, as in our case. There has been work on designing inspection algorithms that plan paths that take into account the viewpoint considerations [33]–[36]. When prior information is available, one can plan inspection paths carefully by taking into account the geometric model of the environment. Typically, the prior information is a low resolution version of the environment and the inspection path can be used to obtain high-resolution measurements of the environment [33], [35]. Unlike these works, we consider a scenario where no prior information is given and the robot must plan on incrementally revealed information.

Bircher et al. [37] presented a receding horizon planner for both the exploration problem as well as the inspection problem. The two algorithms are similar and use a Rapidly-Exploring Random Tree to generate a set of candidate paths in the known, free space of the environment. Then, one amongst these paths is selected based on a criterion that values how much information a path gains about the environment. The planner is used in a receding horizon fashion (repeatedly invoked as new information is gained). We follow a similar approach; however, for the work by Bircher et al., the inspection surface is known a priori. The environment is not necessarily known; they test for both known and unknown. GATSBI has no prior knowledge about either the environment or target inspection surface.

Song et al. [36] recently proposed an online algorithm which consists of a high-level coverage planner and a low-level inspection planner. The low-level planner takes into account the viewpoint constraints and chooses a local path that gains additional information about the structure under inspection. Our work differentiates by guaranteeing a quality of inspection, not requiring a bounding box around the target infrastructure, and segmenting the infrastructure of interest from the environment, guaranteeing inspection of only the target infrastructure.

III. PROBLEM FORMULATION

The overarching problem that we solve in this paper can be described as follows.

Problem 1: Given a UAV with a 3D LiDAR and RGB camera, find a path to inspect every point on the bridge surface so as to minimize the total flight distance.

We consider the scenario where the geometric model of the bridge is unknown a priori. We assume that the UAV is initialized at a location where at least some part of the bridge is visible. We then plan an inspection path for the part of the bridge that is visible. As more of the bridge is seen, we replan. Problem 2 (defined shortly) focuses on finding a path for the UAV based on the partial information. We solve the larger Problem 1 by repeatedly solving Problem 2 as new information is gain.

We use a 3D semantic, occupancy grid to represent the model of the bridge that is built online. Each voxel in the occupancy grid will be assigned a semantic label. The label indicates whether the voxel is free $v_F \in V_F$; is occupied,

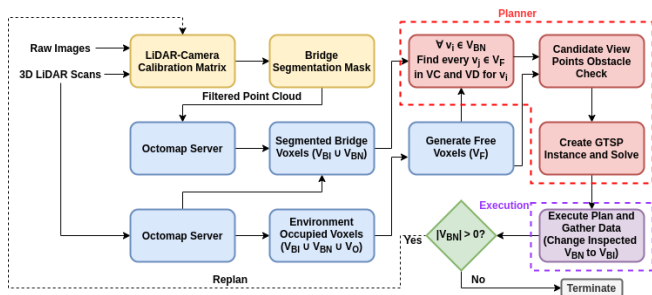


Fig. 2: Flow diagram of GATSBI.

part of the bridge, and previously inspected $v_{BI} \in V_{BI}$; is occupied, part of the bridge, but not yet inspected $v_{BN} \in V_{BN}$; and occupied but not a bridge voxel (i.e., obstacles) $v_O \in V_O$. The free voxels, V_F , represent free space where the UAV can fly. The inspected bridge voxels, V_{BI} , are bridge voxels that have already been inspected by the UAV. The non-inspected bridge voxels, V_{BN} , represent bridge voxels that have been added to the 3D occupancy map, but not yet inspected. Lastly, the obstacle voxels, V_O , represent occupied voxels that are not the bridge in the 3D occupancy map. Our goal is to inspect all the voxels that correspond to the bridge surface, i.e., to ensure that $V_{BN} = \emptyset$.

A voxel $v_{BN} \in V_{BN}$ is said to be inspected if we inspect at least one of its six faces. A face is said to be inspected if the center of that face falls within a cone given apex angle centered at the UAV camera and within a minimum and maximum range of the UAV camera. The apex angle represents the field-of-view of the camera that is rigidly attached to the UAV. The viewing distance is comprised of a minimum and maximum distance that a bridge voxel should be inspected from to ensure quality images for inspection. An example of viewing constraints can be seen in Figure 1, where the green box represents a face of a bridge voxel, the blue cone represents the viewing cone, and the red band on the cone represents the viewing distance. For the rest of the paper, we refer to viewing cone and distance as, *viewP*.

Problem 2: Given a 3D occupancy map consisting of four sets of voxels (V_F, V_{BI}, V_{BN}, V_O), find a minimum length path that inspects every voxel in V_{BN} .

In the following section we show how to model this problem as a GTSP-instance.

IV. THE GATSBI PLANNER

In this section, we give an overview of the GATSBI algorithm. The full pipeline is given in Figure 2 and broadly consists of three modules: perception, planning, and execution. We describe each in details next.

A. Perception

GATSBI starts by segmenting the bridge from the environment using the LiDAR and RGB sensor information. Each incoming image (Figure 3-left) undergoes semantic segmentation to find pixels corresponding to the bridge. In this paper, we use a simple color based segmentation algorithm since we operate in a simulated environment.

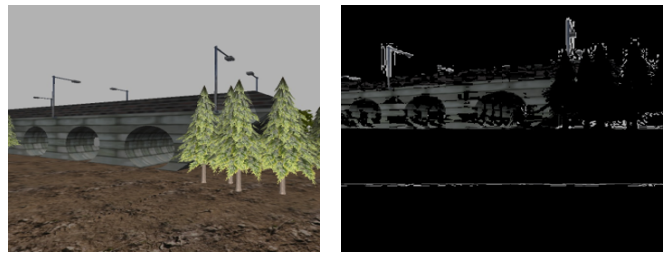


Fig. 3: Left: Single image from the UAV RGB camera. Right: Binary mask created of the image in left.

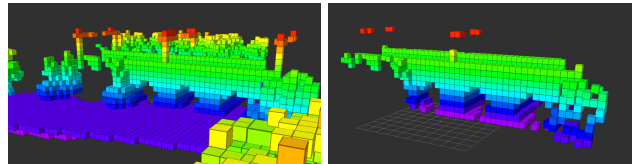


Fig. 4: Left: Full voxel map containing $V_{BI} \cup V_{BN} \cup V_O$. Right: Segmented bridge voxel map containing $V_{BI} \cup V_{BN}$.

However, in recent work [38], we presented a dataset and benchmark of aerial imagery that can be used for training object detectors specifically for bridge inspection tasks.

Using the transformation matrix obtained by extrinsic LiDAR to RGB camera calibration, the LiDAR data is projected onto the image with the binary mask (Figure 3-right). The 3D points that lie on the segmented bridge are classified as bridge points. The point clouds obtained through segmentation are then fed to OctoMap [21] to create a 3D occupancy grid. The output of this module is a set of voxels: free V_F , bridge V_{BI}, V_{BN} , and obstacle V_O . Only the segmented voxels (V_{BI}, V_{BN}) shown in Figure 4-right are used to plan inspection paths. The other voxels V_O and V_F are used only to plan collision-free paths and take into account viewing constraints.

B. Planner

In order to inspect a bridge, we are required to inspect all voxels in V_{BN} (as described in Section III). The planner is repeatedly called over time. The V_{BI} set keeps track of voxels that have been inspected by the UAV previously. This avoids unnecessarily inspecting the same voxel more than once (some are unavoidable). Specifically, each voxel in V_{BN} must be viewed from some point on the path of the UAV within *viewP*. We formulate this problem as a GTSP instance.

The input to GTSP consists of a weighted graph where the vertices are partitioned into clusters. The objective is to find a minimum weight tour that visits at least one vertex in each cluster once. GTSP generalizes the Traveling Salesperson Problem and is NP-Hard [22]. In the following, we describe how we generate the input graph, G , and clusters for GTSP.

Each vertex in G corresponds to a candidate viewpoint. We check all pairs of $v_F \in V_F$ and $v_{BN} \in V_{BN}$ to see if v_F lies within *viewP* of one of the faces of v_{BN} . If so, we add a vertex in the graph G corresponding to the pair v_F and

v_{BN} . This vertex is also added to the cluster corresponding to each v_{BN} .

There can be multiple vertices in G corresponding to the same v_F , but each such voxel will belong to distinct clusters of G . If a v_F does not lie within $viewP$ of any $v_{BN} \in V_{BN}$, then it does not get added to the graph G .

All free voxels that can inspect the same v_{BN} will contribute one vertex each to the cluster corresponding to v_{BN} . The GTSP tour will ensure at least one viewpoint in this cluster is visited.

Next, we create an edge between every pair of vertices in G . The cost for each of these edges is the Euclidean distance between the two vertices. For vertices in the graph G that correspond to the same v_F , the Euclidean distance will equal to zero. With the vertices, edges, and clusters, we create a GTSP instance and use the GTSP solver, GLNS [22], to find a path for the UAV. Note that GTSP will obtain a tour that returns back to the starting vertex (i.e., current position of the UAV). But, we do not need to execute the last edge returning back to the start position of this tour.

C. Execution

We use the navigation planner MoveIt [23] to execute the GTSP path. Prior to moving from one point to the next, we check the distance from the current location of the UAV to the next vertex in the GTSP path. This distance is found using MoveIt [23] which takes into account the obstacles in the occupancy grid. If the difference between this MoveIt distance and the Euclidean distance is greater than DD (discrepancy distance), we replan the GTSP path. We replan as many times as needed to ensure that the first edge in the returned tour is within DD of the MoveIt distance. This is called a lazy evaluation of edge costs. Computing the MoveIt distance (which is a more accurate approximation of the actual travel distances) between every pair of vertices will be time consuming. By checking the discrepancy lazily, we find a tour quickly while also not executing any edge where the actual distance is significantly larger than the expected distance captured by the edge cost.

We keep track of each newly visited cluster during the path flight. Each of these newly visited clusters may correspond to a non-inspected bridge voxel. They are moved from set V_{BN} to V_{BI} since they have now been inspected. We execute the plan until one of two conditions are met: either a time limit (RPT) elapses, or we complete the path, whichever occurs first. We also record the raw sensor data during the flight. The MoveIt planner uses this new data for navigation. Once we complete navigation, we use the stored data to update the bridge inspected and non-inspected voxels and replan. Once V_{BN} is empty, the bridge is considered inspected and GATSBI will terminate.

V. SIMULATIONS

In this section, we present simulation results to evaluate the performance of GATSBI. We first present a qualitative example of the inspection paths produced by GATSBI. Then, we study the effect of varying the parameters on

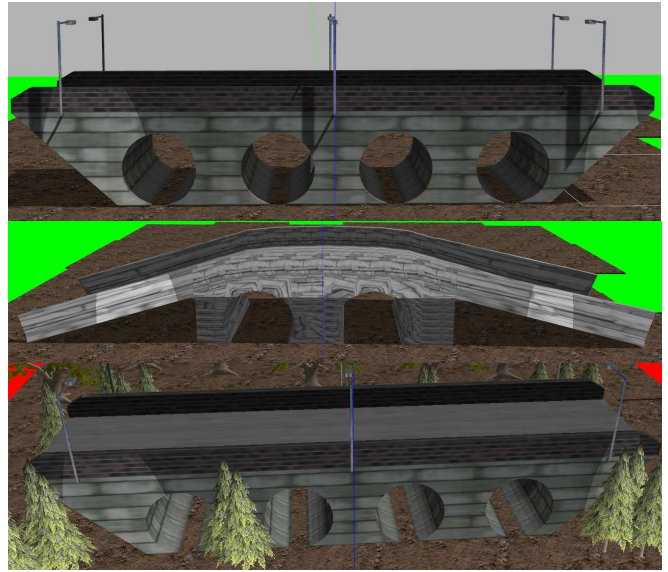


Fig. 5: From top to bottom, bridges 1, 2, and 3.

the performance of the algorithm. We also evaluate the computational time for various subroutines within GATSBI. Finally, we compare GATSBI with the baseline frontier-based exploration.

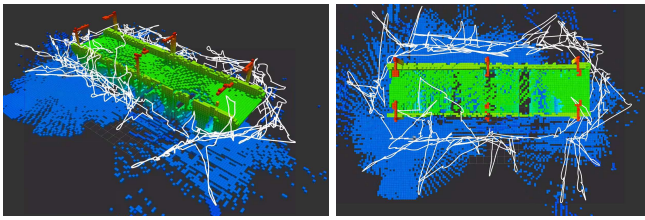
Setup: We use Robot Operating System (ROS) Melodic on Ubuntu 18.04 and Gazebo to carry out the simulations. The simulated UAV is equipped with a Velodyne VLP-16 3D LiDAR and an ASUS Xtion Pro RGB camera. The 3D LiDAR generates around 300,000 points/sec. It also has a 360° horizontal field of view with $\pm 15^\circ$ vertical field of view. The VLP-16 has a range of 100m [39]. The ASUS Xtion Pro has a resolution of 720x480. Its field of view is 58° horizontal, 45° vertical, and 70° diagonal, and the distance that it can be used for is from 0.8m to 3.5m [40].

For all experiments, we use a viewing cone with apex angle of 0° and a viewing distance between 2 to 5 meters. We set the viewing cone to the strictest possibility — a straight line from the camera. This is to ensure the highest quality of images captured for inspection. We set the viewing distance based on [17], where they suggest a minimum flight distance of 2 meters and a maximum of 5 meters to allow for the safe flight of the UAV as well as accurate detection of faults on a bridge.

A. Qualitative Example

We evaluate GATSBI on three bridges shown in in Figure 5. The first two bridges do not contain any other object in the environment except for the ground. The third bridge, on the other hand, has other distractor objects such as the trees. The first and the third bridge are the same model. The second bridge is qualitatively different than the first. Nevertheless, they are all representative of box girder bridges, as in our previous work [18].

Figure 6 shows the path followed by the UAV as given by GATSBI. Figure 7-left shows the final voxel map containing only the V_{BI} voxels. A sample RGB image obtained by the



(a) Angled UAV flight path during GATSBI. (b) Birdseye-view UAV flight path during GATSBI.

Fig. 6: UAV flight paths.

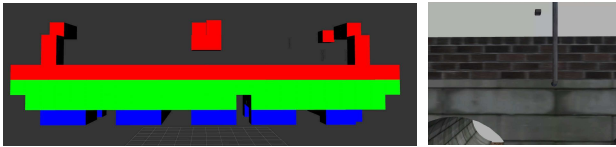


Fig. 7: Outputs from GATSBI. Left: Example output of the voxel map for bridge 1. Right: Example inspection image of bridge 1.

UAV along the path is also shown in Figure 7-right. These results are for bridge 1; the results for the other bridges are comparable. Next we present quantitative results on GATSBI.

B. Effects of Varying the Parameters

Recall that the planner continues as long as $|V_{BN}| \neq 0$. Ideally, this would coincide when all voxels that *can* be inspected, *are* inspected. However, it is possible that the algorithm may terminate if the UAV finishes inspecting all bridge voxels it has seen so far, without having seen the entirety of the bridge. There are two parameters in GATSBI: *replanning trigger time*, RPT , and *distance discrepancy*, DD . In this section, we study the effect of varying these parameters on the performance of the algorithm.

Figure 8 shows the effect of varying RPT on the number of total bridge voxels inspected ($|V_{BI}|$ after the termination of the algorithm) and the total distance traveled by the UAV.

We observe that the number of voxels inspected is not affected by RPT . The distance traveled seems to grow

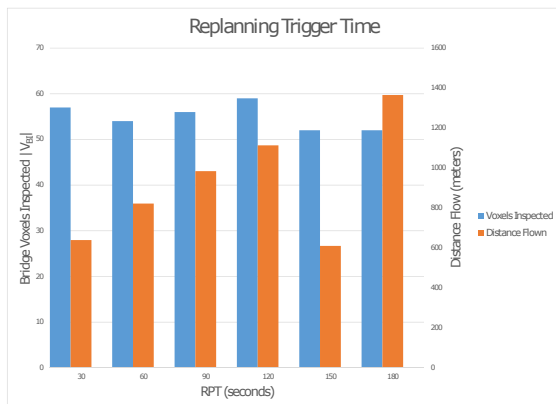


Fig. 8: Evaluation of RPT vs voxels inspected and RPT vs flight distance. We use $RPT = 90$ for all other simulations.

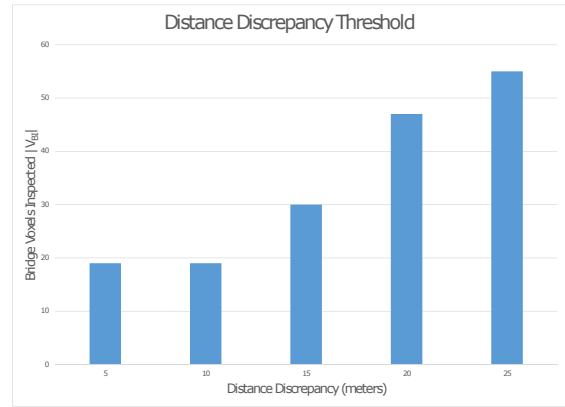


Fig. 9: Evaluation of DD . We use $DD = 25$ for all other simulations.

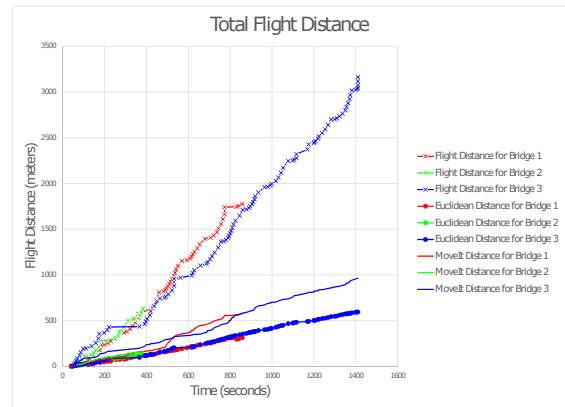


Fig. 10: Travel distances for GATSBI.

linearly with RPT except when $RPT = 150$ seconds. This is expected since larger RPT will let the UAV travel longer before taking into account new information and triggering a replan. A shorter RPT , on the other hand, will force the UAV to replan sooner, therefore leading to better optimized paths. We use $RPT = 90$ for the rest of our simulations.

Figure 9 shows the effect of the total number of bridge voxels inspected as we increase DD . We see a consistent increasing trend. Therefore, we choose $DD = 25$ when comparing the MoveIt distance and the Euclidean distance.

C. Travel Distance

We also evaluate the total distance traveled by the UAV using GATSBI (Figure 10). We report three distances: flight distance, Euclidean distance, and MoveIt distance. The flight distance is computed by recording the actual position of the UAV during the inspection. The Euclidean distance is the straight-line distance between the current position of the UAV and the next point on the path returned by the GTSP solver. The MoveIt distance is the expected travel distance given by MoveIt to the next point.

We observe that the Euclidean and MoveIt distances are comparable to each other (and are bounded by the DD parameter). However, the actual flight distance is larger than the other two. This is likely because during the actual

flight previously unseen obstacles may be seen and need to be avoided; thereby increasing the gap in the actual flight distance and the expected distance.

D. Computational Time

We examine the time it takes for executing GATSBI. In Table I, we report the average, minimum, maximum, and standard deviation (std) of the time for all three bridges. We report three times: the time spent in the planner to create the GTSP instance, the time taken to solve the GTSP instance, and the flight time before the planner is called again. We see that the time it takes GATSBI to perform segmentation and create a GTSP instance takes a maximum of 0.26 seconds. The GTSP solver takes a maximum of 6.15 seconds. Compared to the flight time (average of approximately 50s), the time taken by the planner is not significant. This suggests that GATSBI is not a bottleneck and is capable of running in real-time on UAVs that are executing 3D bridge inspection in unknown environments.

Bridge	Component	Average	Min.	Max.	STD
Bridge 1	non-GTSP	0.06s	0.04s	0.090s	0.02s
Bridge 1	GTSP	5.84s	5.50s	6.00s	0.19s
Bridge 1	Flight	50.49s	7.45s	104.25s	26.50s
Bridge 2	non-GTSP	0.08s	0.05s	0.10s	0.02s
Bridge 2	GTSP	6.05s	5.95s	6.15s	0.08s
Bridge 2	Flight	50.23s	13.22s	101.90s	23.75s
Bridge 3	non-GTSP	0.13s	0.05s	0.26s	0.07s
Bridge 3	GTSP	5.14s	4.79s	5.45s	0.23s
Bridge 3	Flight	50.98s	6.82s	117.23s	27.39s

TABLE I: Table showing the time taken for each part of GATSBI over multiple replans.

E. Comparison with Baseline

We compare the performance of GATSBI with a baseline frontier-based exploration algorithm. Before comparison, we first found the best set of parameters that are used for the baseline method. The results are reported in Appendix I. We tested 3 main parameters. The first was the number of frontiers to visit before planning again. The second was whether to go to the closest frontier or a random frontier. Lastly, we tested the use of a grid parameter. This grid parameter checked whether we had previously visited a frontier in the same grid as the current target frontier. The parameter allowed any number of visits per grid cell from 1 to ∞ (standard frontier exploration). From our evaluations, we find that visiting 10 frontiers before replanning, choosing random frontiers to visit, and having no grid cell visit restrictions is the best combination of parameters.

We compare GATSBI with the baseline method with these chosen parameters. We can see in Figure 11 that our method does better than the baseline method when comparing the percentage of total bridge voxels inspected. We obtain this value by dividing the inspected bridge voxels ($|V_{BI}|$) upon termination of the algorithm by the total bridge voxels. The total number of bridge voxels are obtained by flying the UAV around the bridge and recording the number of bridge voxels. Note that in the third case, this number is greater than

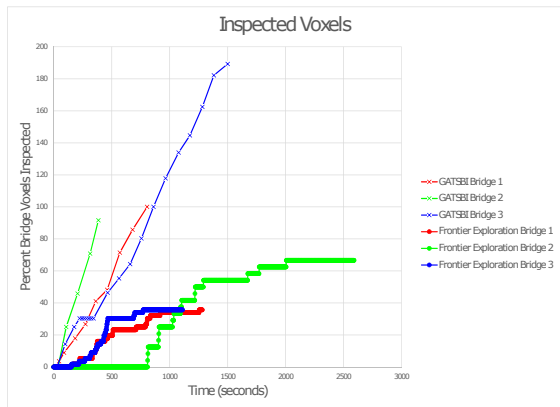


Fig. 11: Percentage of voxels inspected over time for all bridges.

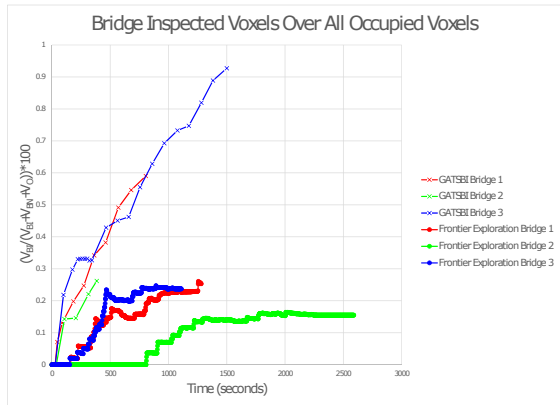


Fig. 12: $|V_{BI}| / (|V_{BI}| + |V_{BN}| + |V_O|)$ over time for all bridges.

100% because of some false positive bridge voxels reported in $|V_{BI}|$.

Nevertheless, we observe that GATSBI achieves inspection of almost 100% voxels while the baseline only achieves a maximum of 35.7%. We also evaluate the efficiency in inspection by computing $|V_{BI}| / (|V_{BI}| + |V_{BN}| + |V_O|)$. This ratio captures the fraction of all bridge inspected voxels over occupied voxels. From Figure 12, we observe that GATSBI always has a higher fraction than the baseline. This validates our claim that GATSBI targets inspection of bridge surfaces instead of just covering the environment. We also see that GATSBI executes inspection faster than the baseline. Therefore, we justify the claim that GATSBI is more efficient in inspection compared to a frontier exploration algorithm.

VI. CONCLUSION

In this paper, we present GATSBI, a method for 3D bridge inspection in an unknown environment. We evaluate the performance of the algorithm through Gazebo simulations with a UAV equipped with a 3D LiDAR and an RGB camera. The simulations show that GATSBI outperforms frontier-based exploration algorithms. In particular, we show that the algorithm is efficient in the sense that it targets voxels that are to be inspected, rather than simply exploring a volume. The

simulations also demonstrate that the algorithm can run in real-time. In future work, we intend to provide theoretical guarantees on the optimality of the algorithm as well as invest in improved segmentation and navigation planners to give us a more accurate representation of the bridge and a more realistic point-to-point plan.

REFERENCES

- [1] Peter Liu, Albert Y Chen, Yin-Nan Huang, J Han, J Lai, S Kang, T Wu, M Wen, and M Tsai. A review of rotorcraft unmanned aerial vehicle (uav) developments and applications in civil engineering. *Smart Struct. Syst.*, 13(6):1065–1094, 2014.
- [2] Tolga Ozaslan, Shaojie Shen, Yash Mulgaonkar, Nathan Michael, and Vijay Kumar. Inspection of penstocks and featureless tunnel-like environments using micro uavs. In *International Conference on Field and Service Robotics*, 2013.
- [3] M. Dunbabin and L. Marques. Robots for environmental monitoring: Significant advancements and applications. *IEEE Robotics and Automation Magazine*, 19(1):24–39, Mar 2012.
- [4] Nathan Michael, Ethan Stump, and Kartik Mohta. Persistent surveillance with a team of mavs. In *Intelligent Robots and Systems (IROS), 2011 IEEE/RSJ International Conference on*, pages 2708–2714. IEEE, 2011.
- [5] Jnaneshwar Das, Gareth Cross, Chao Qu, Anurag Makineni, Pratap Tokekar, Yash Mulgaonkar, and Vijay Kumar. Devices, systems, and methods for automated monitoring enabling precision agriculture. In *Proceedings of IEEE Conference on Automation Science and Engineering*, pages 462–469. IEEE, 2015.
- [6] Pratap Tokekar, Joshua Vander Hook, David Mulla, and Volkan Isler. Sensor planning for a symbiotic UAV and UGV system for precision agriculture. *IEEE Transactions on Robotics*, 2016.
- [7] Tristan Sherman, Joshua Tellez, Tristan Cady, Josue Herrera, Hana Haideri, Jimmy Lopez, Mitchell Caudle, Subodh Bhandari, and Daisy Tang. Cooperative search and rescue using autonomous unmanned aerial vehicles. In *2018 AIAA Information Systems-AIAA Infotech@ Aerospace*, page 1490, 2018.
- [8] Yoonchang Sung and Pratap Tokekar. Algorithm for searching and tracking an unknown and varying number of mobile targets using a limited fov sensor. In *Robotics and Automation (ICRA), 2017 IEEE International Conference on*, pages 6246–6252. IEEE, 2017.
- [9] Inkyu Sa and Peter Corke. Vertical infrastructure inspection using a quadcopter and shared autonomy control. In *Field and service robotics*, pages 219–232. Springer, 2014.
- [10] MA Subhan, AS Bhide, and COEB SSGB. Study of unmanned vehicle (robot) for coal mines. *International Journal of Innovative Research in Advanced Engineering (IJIRAE)*, 1(10):116–120, 2014.
- [11] Luke Yoder and Sebastian Scherer. Autonomous exploration for infrastructure modeling with a micro aerial vehicle. In *Field and service robotics*, pages 427–440. Springer, 2016.
- [12] Tolga Ozaslan, Giuseppe Loianno, James Keller, Camillo J Taylor, Vijay Kumar, Jennifer M Wozencraft, and Thomas Hood. Autonomous navigation and mapping for inspection of penstocks and tunnels with mavs. *IEEE Robotics and Automation Letters*, 2(3):1740–1747, 2017.
- [13] Kostas Alexis, Georgios Darivianakis, Michael Burri, and Roland Siegwart. Aerial robotic contact-based inspection: planning and control. *Autonomous Robots*, 40(4):631–655, 2016.
- [14] Geoffrey A Hollinger, Urbashi Mitra, and Gaurav S Sukhatme. Active classification: Theory and application to underwater inspection. In *Robotics Research*, pages 95–110. Springer, 2017.
- [15] Najib Metni and Tarek Hamel. A uav for bridge inspection: Visual servoing control law with orientation limits. *Automation in construction*, 17(1):3–10, 2007.
- [16] Je-Keun Oh, Giho Jang, Semin Oh, Jeong Ho Lee, Byung-Ju Yi, Young Shik Moon, Jong Seh Lee, and Youngjin Choi. Bridge inspection robot system with machine vision. *Automation in Construction*, 18(7):929–941, 2009.
- [17] Sattar Dorafshan, Marc Maguire, Nathan V Hoffer, and Calvin Coopmans. Fatigue crack detection using unmanned aerial systems in under-bridge inspection. 2017.
- [18] Prajwal Shanthakumar, Kevin Yu, Mandeep Singh, Jonah Orevillo, Eric Bianchi, Matthew Hebdon, and Pratap Tokekar. View planning and navigation algorithms for autonomous bridge inspection with uavs. In *International Symposium on Experimental Robotics (ISER)*, 2018. Accepted.
- [19] B. Kakillioğlu, J. Wang, S. Velipasalar, A. Janani, and E. Koch. 3d sensor-based uav localization for bridge inspection. In *2019 53rd Asilomar Conference on Signals, Systems, and Computers*, pages 1926–1930, 2019.
- [20] Brian Yamauchi. A frontier-based approach for autonomous exploration. In *Proceedings 1997 IEEE International Symposium on Computational Intelligence in Robotics and Automation CIRA'97: Towards New Computational Principles for Robotics and Automation*, pages 146–151. IEEE, 1997.
- [21] Armin Hornung, Kai M. Wurm, Maren Bennewitz, Cyrill Stachniss, and Wolfram Burgard. OctoMap: An efficient probabilistic 3D mapping framework based on octrees. *Autonomous Robots*, 2013. Software available at <http://octomap.github.com>.
- [22] S. L. Smith and F. Imeson. GLNS: An effective large neighborhood search heuristic for the generalized traveling salesman problem. *Computers & Operations Research*, 87:1–19, 2017.
- [23] David Coleman, Ioan Sucan, Sachin Chitta, and Nikolaus Correll. Reducing the barrier to entry of complex robotic software: a moveit! case study. *arXiv preprint arXiv:1404.3785*, 2014.
- [24] Cheng Zhu, Rong Ding, Mengxiang Lin, and Yuanyuan Wu. A 3d frontier-based exploration tool for mavs. In *2015 IEEE 27th International Conference on Tools with Artificial Intelligence (ICTAI)*, pages 348–352. IEEE, 2015.
- [25] Daniel Loubach da Silva Lubanco, Markus Pichler-Scheder, and Thomas Schlechter. A novel frontier-based exploration algorithm for mobile robots. In *2020 6th International Conference on Mechatronics and Robotics Engineering (ICMRE)*, pages 1–5. IEEE, 2020.
- [26] Farzad Niroui, Ben Sprenger, and Goldie Nejat. Robot exploration in unknown cluttered environments when dealing with uncertainty. In *2017 IEEE International Symposium on Robotics and Intelligent Sensors (IRIS)*, pages 224–229. IEEE, 2017.
- [27] Anna Dai, Sotiris Papatheodorou, Nils Funk, Dimos Tzoumanikas, and Stefan Leutenegger. Fast frontier-based information-driven autonomous exploration with an mav. *arXiv preprint arXiv:2002.04440*, 2020.
- [28] Shaojie Shen, Nathan Michael, and Vijay Kumar. Autonomous indoor 3d exploration with a micro-aerial vehicle. In *2012 IEEE international conference on robotics and automation*, pages 9–15. IEEE, 2012.
- [29] Micah Corah, Cormac O’Meadhra, Kshitij Goel, and Nathan Michael. Communication-efficient planning and mapping for multi-robot exploration in large environments. *IEEE Robotics and Automation Letters*, 4(2):1715–1721, 2019.
- [30] Aravind Preshant Premkumar, Kevin Yu, and Pratap Tokekar. Combining geometric and information-theoretic approaches for multi-robot exploration. *arXiv preprint arXiv:2004.06856*, 2020.
- [31] Richard Pito. A solution to the next best view problem for automated surface acquisition. *IEEE Transactions on pattern analysis and machine intelligence*, 21(10):1016–1030, 1999.
- [32] Alberto Quattrini Li. Exploration and mapping with groups of robots: Recent trends. *Current Robotics Reports*, pages 1–11, 2020.
- [33] Cheng Peng and Volkan Isler. Adaptive view planning for aerial 3d reconstruction. In *2019 International Conference on Robotics and Automation (ICRA)*, pages 2981–2987. IEEE, 2019.
- [34] Geoffrey A Hollinger, Brendan Englot, Franz S Hover, Urbashi Mitra, and Gaurav S Sukhatme. Active planning for underwater inspection and the benefit of adaptivity. *The International Journal of Robotics Research*, 32(1):3–18, 2013.
- [35] Mike Roberts, Debadepta Dey, Anh Truong, Sudipta Sinha, Shital Shah, Ashish Kapoor, Pat Hanrahan, and Neel Joshi. Submodular trajectory optimization for aerial 3d scanning. In *Proceedings of the IEEE International Conference on Computer Vision*, pages 5324–5333, 2017.
- [36] Soohwan Song, Daekyum Kim, and Sungho Jo. Online coverage and inspection planning for 3d modeling. *Autonomous Robots*, pages 1–20, 2020.
- [37] Andreas Bircher, Mina Kamel, Kostas Alexis, Helen Oleynikova, and Roland Siegwart. Receding horizon path planning for 3d exploration and surface inspection. *Autonomous Robots*, 42(2):291–306, 2018.
- [38] Eric Loran Bianchi, Lynn Abbott, Pratap Tokekar, and Matt Hebdon. Coco-bridge: Common objects in context. dataset for structural detail detection of bridges. *ASCE Journal of Computing in Civil Engineering*, 2020. <http://coco-bridge.com>.

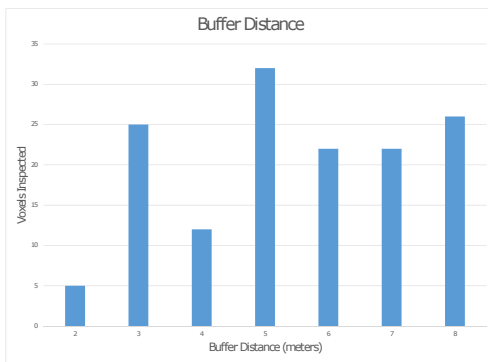


Fig. 13: Evaluating the change of buffer distance from the bridge.

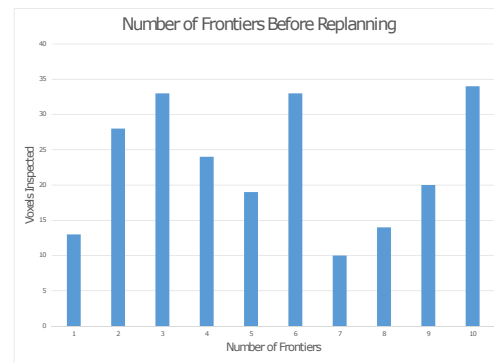


Fig. 14: Evaluation of the number of frontiers the UAV goes to before replanning.

- [39] Velodyne puck vlp-16 sensor — lidar — autonomoustuff. <https://autonomoustuff.com/product/velodyne-puck-vlp-16/>. (Accessed on 09/21/2020).
- [40] Xtion pro — 3d sensor — asus global. https://www.asus.com/3D-Sensor/Xtion_PRO/. (Accessed on 09/22/2020).
- [41] tahsinkose/hector-moveit: Hector quadrotor with moveit! motion planning framework. <https://github.com/tahsinkose/hector-moveit>. (Accessed on 10/16/2020).

APPENDIX I CHOOSING BASELINE PARAMETERS

Frontier-based exploration explores an environment using frontiers, which are free voxels on the boundary of unknown and known space. We consider a general version of frontier exploration where the workspace is divided into a grid with a cell size. The grid size parameter was evaluated in previous work and the size we used, 13x13 cells, was found to have the best results [41]. For potential target frontiers, the algorithm checks whether the robot has previously explored the grid cell the target frontier is in. If it has visited it more than a given threshold, it ignores that frontier and moves onto the next one. This prevents the robot from exploring multiple frontiers in the same vicinity of frontiers that have already been explored.

We create a bounding box surrounding the bridge and restrict the path of the UAV to be inside this box. The parameters that may affect the outcome are the buffer volume surrounding the bridge, the number of frontiers before replanning, the number of voxels per grid cell for the grid-based exploration baseline, and choosing between random vs closest frontiers. In Figure 13, we show the effect of the buffer distance on the ability of the UAV to inspect bridge voxels. We see that a 5 meter buffer gives the best performance.

In Figure 14, we show the effect of varying the number of frontiers that the UAV will visit before replanning. We see that the number of frontiers that the UAV goes to before replanning does not seem to directly affect the number of voxels inspected.

In Figure 15 we evaluate the number of frontiers per grid cell before that grid cell is not visited again. For the grid-based exploration baseline, we settle on 5 frontiers per cell. We can see from the figure that 5 frontiers does the best.

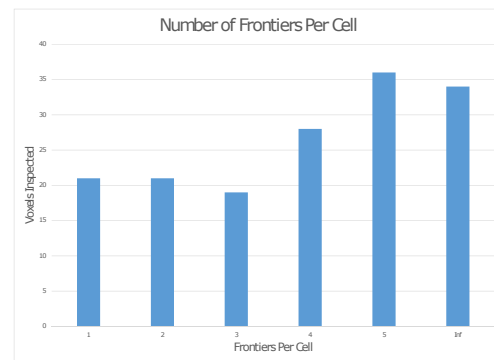


Fig. 15: Evaluation of the number of frontiers per grid if a grid was overlaid on the environment.

The last parameter that we evaluate is whether to choose between random or closest frontier exploration. We can see from Figure 16 that the closest method may provide results faster, but ends up terminating before the random method. Also, the random method does inspect more bridge voxels. Because of this, we do not draw any conclusions between if random or closest is the better method for bridge inspection and choose the random strategy for comparisons with the GATSBI algorithm.

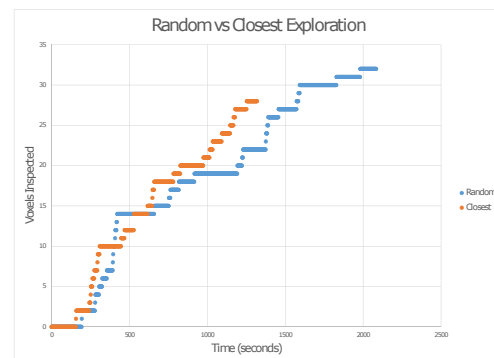


Fig. 16: Comparison of the two methods for choosing frontiers, random or closest.